MFC CDT

University of Southampton

Numerical Analysis - finite difference schemes to solve the advection equation

Lecturer: Hilary Weller

Arianna Ferrotti

November 5, 2024

Contents

Chapter 1

The advection equation

The equation of interest for this analysis is the following hyperbolic one-dimensional partial differential equation, which is the constant-wind-speed advection equation (Durran, 2010):

$$\frac{\partial \phi}{\partial t} + u\frac{\partial \phi}{\partial x} = 0 \tag{1.1}$$

where $\phi = \phi(x, t)$ is the transported quantity, u is the constant flux velocity in the x direction, and (x, t) are the space and time coordinates.
The analytical solution to the equation is known (LeVeque (2002) Chap. 2, Weller (2024*a*)) and it is a translating wave:

$$\phi(x, t) = \phi(x - ut, 0) \tag{1.2}$$

Advection is fundamental in the context of fluid physics as it is used to describe the transport of a conserved quantity (energy and matter) in a flux. Such a quantity can be temperature, humidity, or chemical abundance.

It can thus be used for atmospheric and oceanic modeling. Indeed, advection can contribute to the determination of the impact of greenhouse gas and polluting substances on a global scale, as their distribution is influenced by transport in the atmosphere; heat and humidity are also transported by fluxes of water and air. All this makes advection a key tool to understand the climate termoregulation and simulate the formation of clouds and extreme meteorological events, as well as ocean circulation (Gerdes et al., 1991; Buckley et al., 2015; Holmes et al., 2016).

Chapter 2

Numerical methods

The results presented in this analysis come from the implementation of three finite difference schemes. This means that the derivatives present in Eq. (1.1) are approximated with finite differences, and the numerical solution to the equation is computed on a grid of finite time and space points (Durran (2010) Chap. 3, Jacobson (2005) Chap. 6, Weller (2024*a*)).
In this kind of schemes, the gradients can be approximated with forward, backwards and centered differences.
In the case of time, the first-order forward difference is that between time step n and time step $n+1$ at fixed position x_j, and thus gives for the derivative:

$$\frac{\partial \phi^{(n)}}{\partial t}_j \approx \frac{\phi_j^{(n+1)} - \phi_j^{(n)}}{\Delta t} \tag{2.1}$$

where $\Delta t = t_{n+1} - t_n$ is the time step.
Centered differences in time and space instead give:

$$\frac{\partial \phi^{(n)}}{\partial t}_j \approx \frac{\phi_j^{(n+1)} - \phi_j^{(n-1)}}{2\Delta t} \tag{2.2}$$

for time and:

$$\frac{\partial \phi^{(n)}}{\partial x}_j \approx \frac{\phi_{j+1}^{(n)} - \phi_{j-1}^{(n)}}{2\Delta x} \tag{2.3}$$

for space, where $\Delta x = x_{j+1} - x_j$ is the space resolution. Finally, backwards differences in space will look like:

$$\frac{\partial \phi^{(n)}}{\partial x}_j \approx \frac{\phi_j^{(n)} - \phi_{j-1}^{(n)}}{\Delta x} \tag{2.4}$$

The three schemes in exam are:

- Forward in Time Backwards in Space (FTBS)
- Forward in Time Centered in Space (FTCS)
- Centered in Time Centered in Space (CTCS)

which applied to the advection equation, according to Eq. (2.1-2.4), respectively give:

$$\phi_j^{(n+1)} = \phi_j^{(n)} - c(\phi_j^{(n)} - \phi_{j-1}^{(n)}) \tag{2.5}$$

$$\phi_j^{(n+1)} = \phi_j^{(n)} - c(\phi_{j+1}^{(n)} - \phi_{j-1}^{(n)})/2 \tag{2.6}$$

$$\phi_j^{(n+1)} = \phi_j^{(n-1)} - c(\phi_{j+1}^{(n)} - \phi_{j-1}^{(n)}) \tag{2.7}$$

where $c = u\,\Delta t/\Delta x$ is the Courant number (Weller, 2024*a*).
A scheme like FTBS is said to be upwind when $u \geq 0$, which is always the case in this analysis. These schemes were chosen as they are not difficult to implement, their logic and properties are well described by literature, and they provide an example, when tested and compared one another with simple experiments, of how a different choice of scheme can lead to different results and stability properties.

In the following we will be testing if these methods are bounded and stable, meaning that the errors associated with the numerical approximation do not grow uncontrollably with time, so that the computed solution remains bounded and showing a physical behaviour throughout its evolution (Durran (2010) Chap. 2.1). The *Von Neumann's method* (Weller (2024*c*), Durran (2010) Chap. 3.2.2) allows to predict if a scheme will be stable. Applying it to FTBS, FTCS and CTCS for the advection equation, one finds (Weller, 2024*c*):

- Upwind FTBS stable and damping when $0 \leq c \leq 1$;
- FTCS unconditionally unstable
- CTCS neutrally stable when $-1 \leq c \leq 1$

A scheme that is stable and consistent, i.e. a scheme for which the errors go to zero as the grid spacing goes to zero (LeVeque (2002) Chap. 4.3, Durran (2010) Chap. 2.1), is also convergent, according to the *Lax equivalence theorem* (Lax and Richtmyer (1956), Durran (2010) Chap. 3.2). So another interesting property to check will be the order n at which the errors approach zero as $\Delta x \to 0$. We will thus be evaluating the value of n for which one has that the errors $\sim O(\Delta x^n)$ (Weller (2024*b*), Jacobson (2005) Chap. 6), and that will be the scheme's order of convergence.

Chapter 3

Experiments

This chapter covers the description and results of the tests made on the schemes used. Principally, we look at errors, evaluated as the following ℓ_2-norm, i.e. the integrated differences between the analytical and numerical solution:

$$\ell_2 = \frac{\sqrt{\sum_j \Delta x(\phi_j - f(x_j))^2}}{\sqrt{\sum_j \Delta x\, f(x_j)^2}} \tag{3.1}$$

where Δx is the spatial resolution, j is the spatial index and ϕ_j and $f(x_j)$ are the numerical and analytical solutions at position j (from Weller (2024*c*)).
The tests employed are:

- an analysis of the evolution with time of the errors;
- an analysis of the stability of the schemes, namely the dependence on the Courant number of the errors at the last time step of the computation;
- an analysis of the dependence on the spatial resolution of the errors, which leads to the determination of the order of convergence of the schemes.

In every experiment, the wind-speed is constant and set to $u = 1.0$. The end time of the evolution is also set to 1.0. The number of space points n_x and time steps n_t are set according to the experiment, from which the space and time resolutions are derived as $\Delta x = 1/n_x$ and $\Delta t = 1/n_t$. Then the Courant number is calculated as per definition, i.e. $c = u\Delta t/\Delta x$.
The initial condition is set to be $\phi(x, 0) = \sin^2(2\pi x)$ and the boundary conditions are set to be the same, i.e. $\phi(0, t) = \phi(n_x \Delta x, t)$.

3.1 Errors growth with time

In this case, the computation of the numerical solution is done fixing the parameters of the problem to the following values: $c = 0.4$, $n_x = 50$, $n_t = 125$.
The results for two time steps (one close to halfway of the evolution and one close to the end) are shown in Figure 3.1 for each scheme. This example with $c = 0.4$ is aligned with predictions. In the following, we will discuss these properties more quantitatively, but for the moment these considerations hold: the solution from FTBS reproduces the analytical wave remaining bounded and stable but damping between the two time steps; the FTCS solution instead is amplified, suggesting instability (Durran (2010) Chap. 2.1); finally, CTCS appears as neutrally stable. All this adheres with what discussed in the previous Chapter 2. It is also

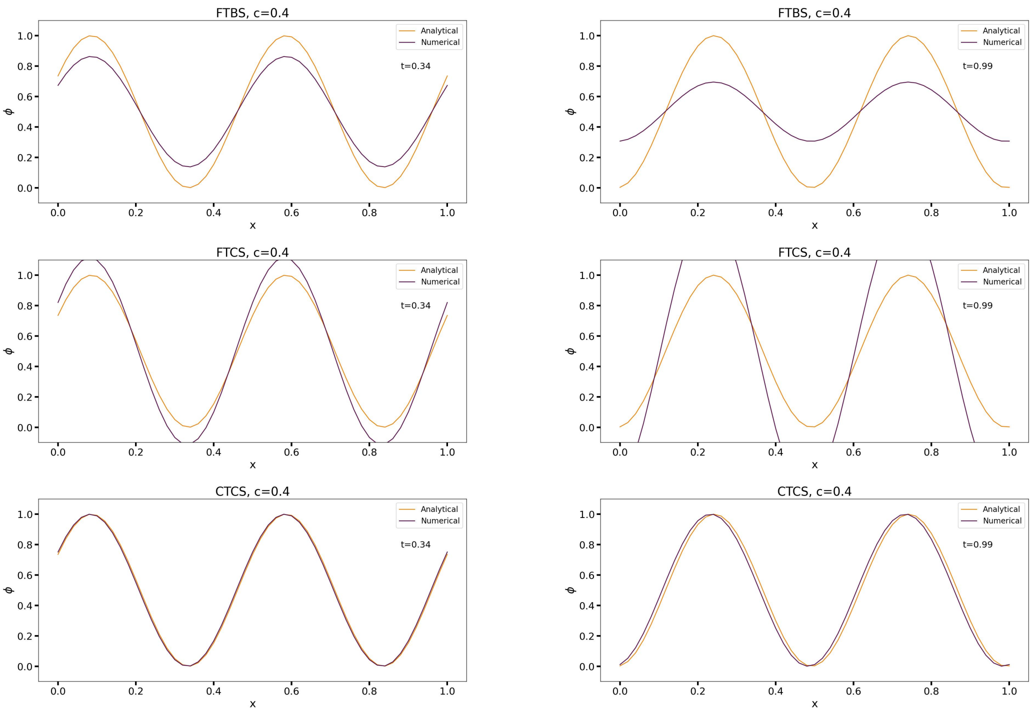

Figure 3.1: Comparison between the analytical (orange wave) and numerical (purple wave) solutions, for the three different schemes (rows from up to bottom: FTBS, FTCS and CTCS). The numerical solution was obtained taking Courant number c=0.4, 125 time steps and spatial resolution $\Delta x = 1/50$. **Left column**: Solutions computed at t=0.34, i.e. after 40 time steps from the beginning of the evolution. **Right column**: Solutions computed at t=0.99, i.e. at 3 time steps from the end of the evolution.

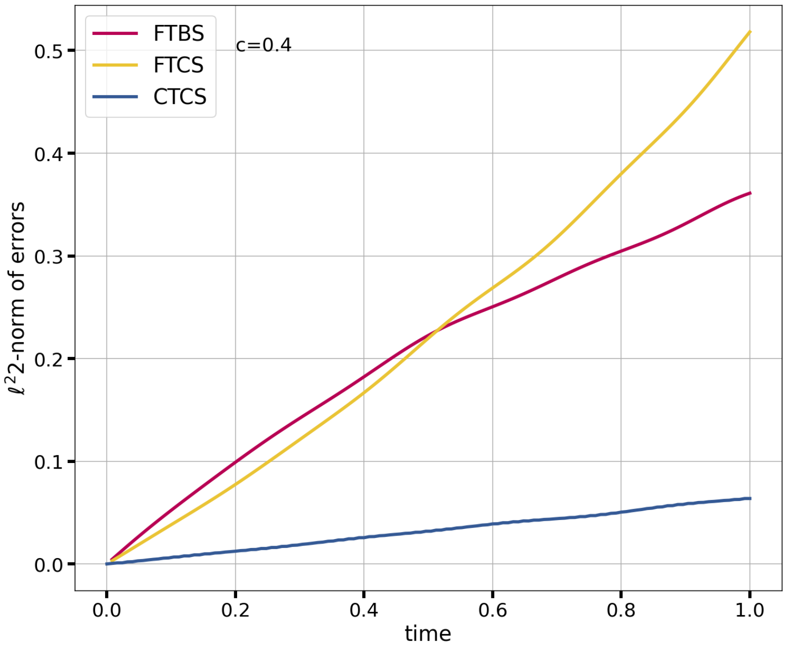

Figure 3.2: Evolution with time elapsed from the initial condition of the ℓ_2-norm of the difference between the analytical and numerical solution, for the three finite difference schemes: FTBS (magenta line), FTCS (yellow line) and CTCS (blue line).

slightly noticeable that the propagation is affected by numerical dispersion when the wave is advected by CTCS (bottom right panel), as the phase speed has decreased (Weller, 2024*d*).

To better evaluate if these considerations hold for all the evolution as expected, the ℓ_2-norm of the integrated difference between the analytical and numerical solution (Eq. (3.1)) is then computed at every time step. When seen with respect to the time elapsed from the initial condition, as in Figure 3.2, it shows clearly the increasing discrepancy, that can be found in all of the finite differences methods, due to the accumulated time discretisation error. Indeed, because of this, all schemes progressively diverge from the actual solution of the equation. But, while FTBS and CTCS (the magenta and blue lines) give errors that seem to grow linearly, or at least with downwards concavity (which would imply boundness), the yellow line shows an unbounded growth of the errors given by the FTCS scheme, due to its intrinsic amplification, and implying instability (Weller, 2024*c*).
Finally, the intersection between the yellow and magenta lines (at $t \approx 0.5$) seems to suggest an interesting property, but at the moment we have not found a theoretical explanation, nor we can say for certainty that it is actually a property that can be generalised and predicted.

3.2 Stability of the schemes

To check that the schemes implemented satisfy the stability conditions predicted from theoretical calculations (see *Von Neumann's analysis* in Chapter 2), it is useful to see how the errors computed as in Eq. (3.1) vary with the Courant number c, which in this example is taken from a grid of 100 values that go from 0.1 to 1.4. The numerical solution is then computed by fixing the space resolution to $\Delta x = 1/60$ and the number of time steps to $n_t = 60$, and taking, for every run, a different value of c from its grid. Then the errors are

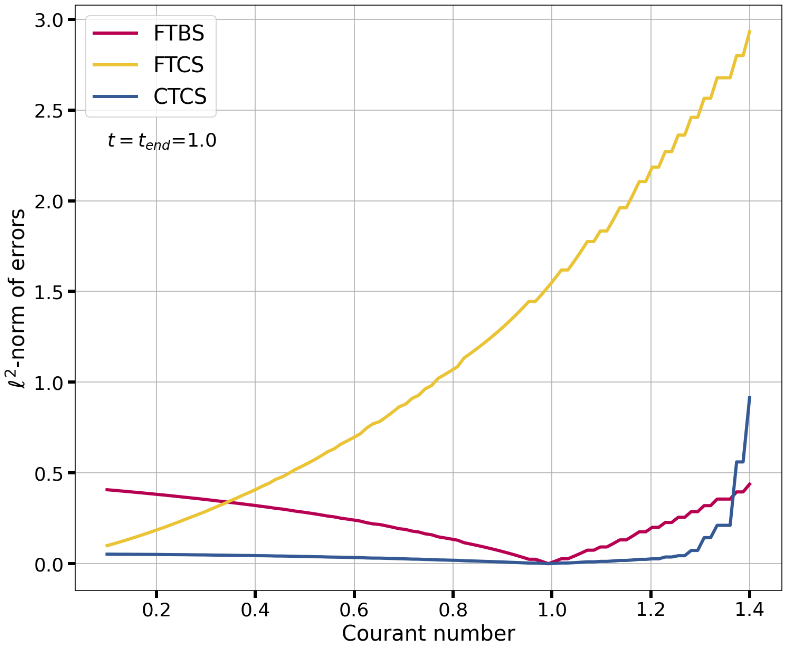

Figure 3.3: Dependence on the Courant number c of the ℓ_2-norm of the difference between the analytical and numerical solution, for the three finite difference schemes: FTBS (magenta line), FTCS (yellow line) and CTCS (blue line).

evaluated at $t = t_{end} = 1.0$ as the ℓ_2-norm of the integrated difference between the analytical and numerical solution (Eq. (3.1)), and they are shown against the grid of values for c in Figure 3.3. It can be seen that the errors remain small and almost constant with c when advecting with CTCS, as expected from the result for which CTCS is unconditionally stable when $|c| \leq 1$ (Chap. 2), and it appears that the errors start to grow for greater values of c. The line for FTBS (in magenta) shows a downward concavity as it approaches null errors when $c = 1$. This agrees with the prediction for which FTBS is stable but damping as long as $0 < c < 1$, and suggests that the damping decreases for increasing c in this range, reaching neutral stability for $c = 1$.
On the other hand, errors from FTCS are not bounded in any range of values of the Courant number, implying, as expected, unconditional instability for FTCS.

3.3 Order of convergence for stable schemes

As the previous analysis and references conclude that FTCS is unstable (and thus not consistent), the following test is carried out only for the FTBS and CTCS schemes. In this case, the ℓ_2-norm of the errors (Eq. (3.1)) is computed at the last time step (where errors have accumulated), so for $t = t_{end} = 1.0$, varying the spatial resolution and keeping the Courant number fixed to $c = 0.4$. Values of n_x are taken from the sequence [30,40,50,60,70,80] and the time steps are computed accordingly (as n_x/c), wanting to keep the end time at 1.0 and the Courant number fixed.
The results are shown in Figure 3.4 versus the space resolution $\Delta x = 1/n_x$. The plane is log-log as this allows to clearly see and compute the order n of growth $\sim O(\Delta x^n)$, namely the order of convergence, which can be calculated as the slope of the linear fit to the points (Weller, 2024*b*).
The linear trends suggest that the errors do converge to 0 when the resolution in space

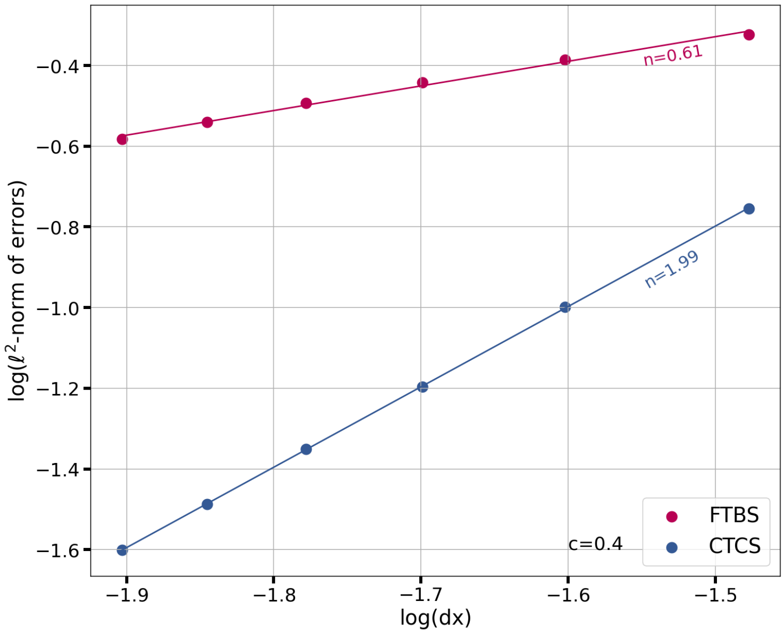

Figure 3.4: Dependence on spatial resolution of the ℓ_2-norm of the difference between the analytical and numerical solution for FTBS (magenta points) and CTCS (blue points). Respective linear fits (obtained through the function `curve_fit` from the `scipy.optimize` PYTHON package) are also shown, and the slope n for both fits is marked.

and time are increased, and particularly that this goes as $\sim O(\Delta x^{0.61})$ for FTBS and as $\sim O(\Delta x^{1.99})$ for CTCS. The result for CTCS is as expected from theoretical computations, i.e. $n = 2$ (Weller (2024*b*), Jacobson (2005), Chap. 6), whereas FTBS seems to converge too slowly, as we would expect errors(FTCS) $\sim O(\Delta x)$. As all the standard procedures have been implemented, this difference seems to suggest that there are other factors at play that haven't been taken fully into account, contributing to a higher rate of error growth for FTBS.

Chapter 4

Conclusions

The advection equation (Eq. (1.1)) is a simple and yet interesting example on which to test numerical schemes. It provides many opportunities to turn the theory into practice when learning about numerical analysis. Given that the analytical solution to this equation is known (Eq. (1.2)), the errors, stability and convergence of schemes can be verified easily.

In this work, we implemented three finite difference schemes (FTBS, FTCS and CTCS, see Chapter 2) to solve numerically the advection equation. We then carried out stability and accuracy tests (Chapter 3) to check if our outcome followed the properties that are predicted from the theory of numerical analysis for these schemes.

The tests regarding boundness and stability of the solution produce results that agree with the theoretical predictions, for example with the unconditional (from the value of the Courant number) instability of FTCS and neutral stability of CTCS (Figure 3.3). Finally, the test on the order of convergence does give a very close-to-expectations value for CTCS (which theoretically goes as $\sim O(\Delta x^2)$ and we obtain $n = 1.99$), whereas it returns a too little ($n = 0.61$) value for FTBS, which would be expected to converge linearly to 0 as Δx does. We concluded that there might be factors at play that haven't been taken fully into account (mostly due to lack of time, unfortunately), and that contribute to a higher rate of error in that case.

With more to learn on this subject and more occasions to test, it could be interesting to see what is causing this higher rate, for example considering different numbers of space points and time steps, as well as checking the amplification factors. Also, running the evolution of the wave for longer times would allow to see when errors saturate and if the considerations on stability and boundness would still hold. And surely, many more conditions could be checked, and more quantitative considerations could be reached. For example, finding a theoretical expression for the errors growth with the time elapsed from the initial condition, to maybe explain the apparent overtake of FTCS over FTBS (intersection in Figure 3.2), and possibly predict it.

References

Buckley, M. W., Ponte, R. M., Forget, G. and Heimbach, P. (2015), 'Determining the origins of advective heat transport convergence variability in the north atlantic', *Journal of Climate* **28**(10), 3943–3956.

Durran, D. (2010), *Numerical Methods for Fluid Dynamics: With Applications to Geophysics*, Texts in Applied Mathematics, Springer New York.
URL: *https://books.google.co.uk/books?id=ThMZrEOTuuUC*

Gerdes, R., Köberle, C. and Willebrand, J. (1991), 'The influence of numerical advection schemes on the results of ocean general circulation models', *Climate Dynamics* **5**, 211–226.

Holmes, C. R., Woollings, T., Hawkins, E. and De Vries, H. (2016), 'Robust future changes in temperature variability under greenhouse gas forcing and the relationship with thermal advection', *Journal of Climate* **29**(6), 2221–2236.

Jacobson, M. Z. (2005), *Fundamentals of Atmospheric Modeling*, 2 edn, Cambridge University Press.

Lax, P. D. and Richtmyer, R. D. (1956), 'Survey of the stability of linear finite difference equations', *Communications on Pure and Applied Mathematics* **9**(2), 267–293.
URL: *https://onlinelibrary.wiley.com/doi/abs/10.1002/cpa.3160090206*

LeVeque, R. (2002), *Finite Volume Methods for Hyperbolic Problems*, Cambridge Texts in Applied Mathematics, Cambridge University Press.
URL: *https://books.google.co.uk/books?id=QazcnD7GUoUC*

Weller, H. (2024*a*), 'Chapter 1: Finite differences for solving pdes'.

Weller, H. (2024*b*), 'Chapter 2: Taylor series and order of accuracy'.

Weller, H. (2024*c*), 'Chapter 5: Stability analysis'.

Weller, H. (2024*d*), 'Chapter 6: Waves, dispersion and dispersion errors'.